

RESEARCH ARTICLE | *Inflammation, Immunity, Fibrosis, and Infection*

# MMP-9-induced increase in intestinal epithelial tight permeability is mediated by p38 kinase signaling pathway activation of MLCK gene

Rana Al-Sadi,<sup>1</sup> Moustafa Youssef,<sup>2</sup> Manmeet Rawat,<sup>2</sup> Shuhong Guo,<sup>2</sup> Karol Dokladny,<sup>2</sup> Mohammad Haque,<sup>1</sup> Martin D. Watterson,<sup>3</sup> and Thomas Y. Ma<sup>1,2</sup>

<sup>1</sup>Penn State Milton S. Hershey Medical Center, College of Medicine, Hershey, Pennsylvania; <sup>2</sup>Department of Internal Medicine, University of New Mexico School of Medicine, Albuquerque, New Mexico; and <sup>3</sup>Drug Discovery Program, Northwestern University, Chicago, Illinois

Submitted 16 April 2018; accepted in final form 7 December 2018

**Al-Sadi R, Youssef M, Rawat M, Guo S, Dokladny K, Haque M, Watterson MD, Ma TY.** MMP-9-induced increase in intestinal epithelial tight permeability is mediated by p38 kinase signaling pathway activation of MLCK gene. *Am J Physiol Gastrointest Liver Physiol* 316: G278–G290, 2019. First published December 13, 2018; doi:10.1152/ajpgi.00126.2018.—Matrix metalloproteinase-9 (MMP-9) has been implicated as being an important pathogenic factor in inflammatory bowel disease (IBD). MMP-9 is markedly elevated in intestinal tissue of patients with IBD, and IBD patients have a defective intestinal tight-junction (TJ) barrier manifested by an increase in intestinal permeability. The loss of intestinal epithelial barrier function is an important contributing factor in the development and prolongation of intestinal inflammation; however, the role of MMP-9 in intestinal barrier function remains unclear. The purpose of this study was to investigate the effect of MMP-9 on the intestinal epithelial TJ barrier and to delineate the intracellular mechanisms involved by using in vitro (filter-grown Caco-2 monolayers) and in vivo (mouse small intestine recycling perfusion) systems. MMP-9 caused a time- and dose-dependent increase in Caco-2 TJ permeability. MMP-9 also caused an increase in myosin light-chain kinase (MLCK) gene activity, protein expression, and enzymatic activity. The pharmacological MLCK inhibition and siRNA-induced knockdown of MLCK inhibited the MMP-9-induced increase in Caco-2 TJ permeability. MMP-9 caused a rapid activation of the p38 kinase signaling pathway and inhibition of p38 kinase activity prevented the MMP-9-induced increase in MLCK gene activity and the increase in Caco-2 TJ permeability. MMP-9 also caused an increase in mouse intestinal permeability in vivo, which was accompanied by an increase in MLCK expression. The MMP-9-induced increase in mouse intestinal permeability was inhibited in MLCK-deficient mice. These data show for the first time that the MMP-9-induced increase in intestinal TJ permeability in vitro and in vivo was mediated by the p38 kinase signal transduction pathway upregulation of MLCK gene activity and that therapeutic targeting of these pathways can prevent the MMP-9-induced increase in intestinal TJ permeability.

**NEW & NOTEWORTHY** MMP-9 is highly elevated in patients with IBD. IBD patients have compromised intestinal TJ barrier function manifested by an increase in intestinal permeability and intestinal inflammation. This study shows that MMP-9, at clinically achievable concentrations, causes an increase in intestinal TJ permeability in vitro and in vivo. In addition, a MMP-9-induced increase in intestinal TJ permeability was mediated by an increase in MLCK gene and protein expression via the p38 kinase pathway.

## INTRODUCTION

Intestinal epithelial tight junctions (TJ) are apicalmost junctional complexes and act as a functional and structural barrier against paracellular permeation of harmful luminal antigens that can promote intestinal inflammation (24, 33). The defective intestinal TJ barrier is a key pathogenic factor contributing to the development of intestinal inflammation in inflammatory bowel disease (IBD), including Crohn's disease (CD) and ulcerative colitis (UC) and other inflammatory conditions of the gut (25, 47). Clinical studies in IBD patients have shown that a persistent increase in intestinal permeability is predictive of a poor clinical outcome and that normalization of intestinal permeability correlates with a sustained long-term clinical remission (52, 54). Similarly, in animal models of IBD, enhancement of the intestinal TJ barrier protects against the development of intestinal inflammation (28), (6), (41).

Matrix metalloproteinases (MMPs) are Zn<sup>2+</sup>-dependent endopeptidases that are engaged in the degradation and remodeling of extracellular matrix (ECM) and regulate ECM homeostasis (9, 39). Under normal physiological conditions, MMPs play a critical role in tissue remodeling and wound repair. However, dysregulated expression of MMPs also plays an important pathogenic role in a number of inflammatory diseases, including arthritis, atherosclerosis, myocardial infarction, colorectal cancer, tumor invasion, and IBD (17, 27, 49). MMP-9 levels are markedly elevated in intestinal tissue, serum, and stool of patients with IBD and closely correlate with the disease activity and degree of inflammation (19, 29). In animal models of IBD, MMP-9-deficient (MMP-9<sup>-/-</sup>) mice are protected from intestinal inflammation (10). Previous studies have shown that MMP-9 levels are upregulated during experimental colitis in mice in response to luminal toxin (dextran sodium sulfate, DSS) as well as bacteria *Salmonella enterica serovar* Typhimurium (S.T.) (10, 26, 46). MMP-9<sup>-/-</sup> mice exposed to DSS or S.T. had dramatically reduced inflammation and mucosal injury (22, 40). In the Caco-2 intestinal cell line, MMP-9 has been shown to inhibit cell adhesion and wound repair (10). In transgenic mice, the expression of MMP-9 in the intestinal epithelium was also associated with an increase in proinflammatory chemokines and an increase in intestinal inflammation following DSS administration (32). MMP-9 gene deletion or pharmacological inhibition of MMP-9 prevented the intestinal inflammation in a mouse model of enterocolitis (38). Similarly, Garg et al. (22)

Address for reprint requests and other correspondence: T. Y. Ma, Penn State Milton S. Hershey Medical Center, 500 University Dr., Rm. 6840, Hershey, PA 17033 (e-mail: thomasma@pennstatehealth.psu.edu).

showed that MMP-9 was responsible for the inflammatory response and tissue damage in mouse models of colitis. Collectively, these studies demonstrated that the increased intestinal expression of MMP-9 was an important contributing factor in the development of intestinal inflammation. Although the defective intestinal epithelial TJ barrier is an important pathogenic factor of IBD and the development of intestinal inflammation, the role of MMP-9 in intestinal TJ barrier function remained unclear. Therefore, the aim of this study was to investigate the effects of clinically relevant concentrations of MMP-9 on intestinal epithelial TJ barrier function and to delineate the potential mechanisms involved by using an *in vitro* cell culture model of intestinal epithelium and an *in vivo* model in live mice. Our results show that MMP-9 causes an increase in intestinal epithelial TJ permeability *in vitro* and *in vivo* and that the increase is mediated by the p38 kinase targeting of myosin light-chain kinase (MLCK) gene expression and activity.

## MATERIALS AND METHODS

**Reagents.** DMEM, trypsin, FBS, glutamine, penicillin, streptomycin, PBS, horseradish peroxidase (HRP)-conjugated secondary antibodies for Western blot analysis were purchased from Invitrogen Life Technologies (San Francisco, CA). Phospho-p38 kinase, MLCK, and anti- $\beta$ -actin antibodies and ML-7 and SB-208530 were obtained from Sigma (St. Louis, MO). siRNA of MLCK, p38 kinase, and transfection reagents were from Dharmacon (Lafayette, CO). The active form of MMP-9 was purchased from Abcam (Cambridge, MA), isolated from stimulated human neutrophil granulocytes, disulfide-bridged MMP-9 homodimer. The pro-domain embraces a conserved "cysteine switch" sequence motif in close proximity to the border zone of the catalytic domain, whose free cysteine residue interacts with the catalytic zinc ion to maintain enzyme latency and prevent binding and cleavage of the substrate. Activation of the MMP zymogen depends on a conformational change in the pro-domain, which pulls out the cysteine residue and enables water to interact with the zinc ion in the active site. A human MMP-9 ELISA kit was purchased from Sigma-Aldrich (St. Louis, MO). All other chemicals were of reagent grade and were purchased from Sigma-Aldrich (St. Louis, MO), VWR (Aurora, CO), or Fisher Scientific (Pittsburgh, PA).

**Cell culture.** Caco-2 cells (passage 20) were purchased from the American Type Culture Collection (Manassas, VA) and maintained at 37°C in a culture medium composed of DMEM with 4.5 mg/ml glucose, 50 U/ml penicillin, 50 U/ml streptomycin, 4 mM glutamine, 25 mM HEPES, and 10% FBS. The cells were kept at 37°C in a 5% CO<sub>2</sub> environment. Culture medium was changed every 2 days. The cells were subcultured by partial digestion with 0.25% trypsin and 0.9 mM EDTA in Ca<sup>2+</sup>-free and Mg<sup>2+</sup>-free PBS. For growth on filters, high-density Caco-2 cells (1 × 10<sup>5</sup> cells) were plated on Transwell filters with 0.4- $\mu$ m pore (Corning, Corning, NY) and monitored regularly by visualization with an inverted microscope (Eclipse TS100/100-F; Nikon, Melville, NY) and by epithelial resistance measurements. The human intestinal Caco-2 cell line has been used extensively over the last 20 years as *in vitro* model system of functional epithelial barriers.

**Determination of epithelial monolayer resistance and paracellular permeability.** The transepithelial electrical resistance (TER) of the filter-grown Caco-2 intestinal monolayers was measured using an epithelial voltohmmeter (EVOM; World Precision Instruments, Sarasota, FL) as previously reported (4, 55). After treatment including MMP-9 (MMP-9 was refreshed every 24 h), ML-7 and siRNA, both apical and basolateral sides of the epithelium, were bathed with DMEM. Electrical resistance was measured in 5% difference on three consecutive measurements. Caco-2 monolayer paracellular permeability

was determined using inulin, an established paracellular marker (4, 5, 55). Unless specified otherwise, DMEM (pH 7.4) was used as the incubation solution during the experiments. Buffered solution (0.5 ml) was added to the apical compartment, and 1.5 ml was added to the basolateral compartment to ensure equal hydrostatic pressure, as recommended by the manufacturer. Known concentrations of permeability marker inulin (10  $\mu$ M) and its radioactive tracer were added to the apical solution. Low concentrations of permeability marker were used to ensure that negligible osmotic or concentration gradient was introduced. All flux studies were carried out at 37°C. For determination of mucosal-to-serosal flux rates of inulin, Caco-2-plated filters having epithelial resistance of 400–550  $\Omega$ -cm<sup>2</sup> were used. All of the permeability experiments were repeated three to four times in triplicate.

**Assessment of protein expression by Western blot analysis.** Protein expression from Caco-2 cells and mouse tissue was assessed by Western blot analysis, as previously described. Cells and mouse tissue were lysed with lysis buffer (50 mM Tris-HCl, pH 7.5, 150 mM NaCl, 500  $\mu$ M NaF, 2 mM EDTA, 100  $\mu$ M vanadate, 100  $\mu$ M PMSF, 1  $\mu$ g/ml leupeptin, 1  $\mu$ g/ml pepstatin A, 40 mM paranitrophenyl phosphate, 1  $\mu$ g/ml aprotinin, and 1% Triton X-100) on ice for 30 min. The lysates were centrifuged at 10,00 *g* for 10 min in an Eppendorf centrifuge (5417R; Hauppauge, NY) to obtain a clear lysate. The supernatant was collected and protein concentration was determined using the Bio-Rad Protein Assay kit (Bio-Rad, Hercules, CA). Laemmli gel loading buffer (Bio-Rad) was added to the lysate containing 10–20  $\mu$ g of protein and boiled at 100°C for 7 min, after which proteins were separated on an SDS-PAGE gel. Proteins from the gel were transferred to the membrane (Trans-Blot Transfer Medium, Nitrocellulose Membrane, Bio-Rad) overnight. The membrane was incubated for 2 h in blocking solution (5% dry milk in TBS-Tween-20 buffer) and then incubated with antibody in blocking solution. After a wash in TBS-1% Tween buffer, the membrane was incubated in secondary antibody and developed using Western Blotting Luminol Reagents (Santa Cruz Biotechnology, Santa Cruz, CA) on Kodak BioMax MS film (Fisher Scientific). The films were exposed for between 5 s and 10 min.

**siRNA of p38 kinase and MLCK.** Targeted siRNAs were obtained from Dharmacon (Chicago, IL). Caco-2 monolayers were transiently transfected using DharmaFect transfection reagent (Lafayette). Briefly, 5 × 10<sup>5</sup> cells per filter were seeded into a 12-well transwell plate and grown to confluence. Caco-2 monolayers were then washed twice with PBS and 1.0 ml of Opti-MEM was added to the apical compartment of each filter and 1.5 ml was added to the basolateral compartment of each filter. Five nanograms of the siRNA of interest and 2  $\mu$ l of DharmaFect reagent were preincubated in Opti-MEM. After 5 min of incubation, the two solutions were mixed and incubated for another 20 min, and the mixture was added to the apical compartment of each filter. The MMP-9 experiments were carried out 96 h after transfection. The efficiency of silencing was confirmed by Western blot analysis.

**ELISA-based *in vitro* p38 kinase activity.** As previously described (2), activating transcription factor 2 (ATF-2) was diluted in PBS and coated on streptavidin 96-well plates at 37°C for 1 h. The plates were washed three times with PBS, incubated with blocking solution (1 mg/ml bovine serum albumin in PBS) at 37°C for 1 h, and then washed three times with PBS. The kinase reaction buffer (90  $\mu$ l; 20 mM Tris-HCl, pH 7.5, 10 mM MgCl<sub>2</sub>, 50 mM NaCl, 1 mM DTT, 1 mM NaF, 50  $\mu$ M ATP) provided by the manufacturer (MBL International, Woburn, MA), the samples containing immunoprecipitated p38 kinase (10  $\mu$ l) were added to each well, and the kinase reaction (phosphorylation of ATF-2) was carried out at 37°C for 30–60 min. The reaction was stopped by removing the reaction mixtures and washing the plates three times with washing buffer (20 mM Tris-HCl at pH 7.4, 0.5 M NaCl, and 0.05% Tween 20). The washed plates were incubated with the anti-phospho-ATF-2 antibody (5 ng/ml) at room temperature for 1 h. The plates were then washed four times with washing buffer, and goat anti-rabbit IgG antibody (diluted at 1:2,000

in washing buffer) was added to the wells, and the plates were incubated at 37°C for 1 h. The plates were then washed four times and incubated with 100- $\mu$ l substrate solution tetramethylbenzidine at 37°C for 5–15 min. A stop solution containing 0.5 N H<sub>2</sub>SO<sub>4</sub> (100  $\mu$ l) was added to stop the reaction. Absorbance at 450 nm was determined using the SpectraMax 190 (Molecular Devices).

**ELISA-based MLCK *in vitro* kinase activity.** As previously described (4), biotinylated MLC was diluted in PBS and coated on streptavidin 96-well plates at 37°C for 1 h. The plates were washed three times with PBS, incubated with blocking solution (1 mg/ml BSA in PBS) at 37°C for 1 h, and then washed three times with PBS. The kinase reaction buffer (90  $\mu$ l), provided by the manufacturer (MBL International, Woburn, MA) and the treated samples (10  $\mu$ l) were added to the wells, and the kinase reaction (MLC phosphorylation) was performed at 37°C for 30–60 min. The reaction was stopped by removing the reaction mixtures and washing the plates three times with buffer (20 mM Tris-HCl at pH 7.4, 0.5 M NaCl, and 0.05% Tween 20). The washed plates were incubated with the anti-phospho-MLC-S19 antibody (5 ng/ml, Cat: M6068, Sigma-Aldrich) at room temperature for 1 h, after which the plates were washed four times with buffer. HRP-goat anti rabbit IgG (diluted at 1:2,000 in washing buffer) was added to the wells and the plates were incubated at 37°C for 1 h. The plates were washed four times and then incubated with 100  $\mu$ l substrate solution (tetramethylbenzidine) for 5–15 min at 37°C. The reaction was stopped by adding 100  $\mu$ l of 0.5 N H<sub>2</sub>SO<sub>4</sub>. The absorbance at 450 nm was determined using the SpectraMax 190 (Molecular Devices, Sunnyvale, CA).

**RNA isolation and reverse transcription.** Caco-2 cells ( $5 \times 10^5$  cells per filter) were seeded into 12-well Transwell permeable inserts and grown to confluence. Filter-grown Caco-2 cells were then treated with MMP-9. At the end of the experimental period, cells were washed with ice-cold PBS. Total Caco-2 RNA was isolated using a Qiagen RNeasy Kit (Valencia, CA) according to the manufacturer's protocol. Total RNA concentration was determined by absorbance at 260/280 nm using the SpectraMax 190 (Molecular Devices). Reverse transcription (RT) was carried out using the GeneAmp Gold RNA PCR core kit (Applied Biosystems, Carlsbad, CA). Total RNA (2 ng) from each sample was reverse-transcribed into cDNA in a 40- $\mu$ l reaction (containing  $1 \times$  RT-PCR buffer, 2.5 mM MgCl<sub>2</sub>, 250  $\mu$ M of each dNTP, 20 U of RNase inhibitor, 10 mM DTT, 1.25  $\mu$ M random hexamer, and 30 U of multiscribe RT). RT reactions were performed in a thermocycler (PTC-100; MJ Research, Waltham, MA) at 25°C for 10 min, 42°C for 30 min, and 95°C for 5 min.

**Quantification of gene expression using real-time PCR.** The real-time PCRs were conducted using the ABI prism 7900 sequence detection system and TaqMan universal PCR master mix kit (Applied Biosystems) as previously described (36). Each real-time PCR contained 10  $\mu$ l of RT reaction mix, 25  $\mu$ l  $2 \times$  TaqMan universal PCR master mix, 0.2  $\mu$ M probe, and 0.6  $\mu$ M primers. Primer and probe design for the real-time PCR was made with Primer Express v. 2 (Applied Biosystems). MLCK-specific primer pairs consisted of 5'-AGGAAGGCAGCATTGAGGTTT-3' (forward), 5'-GCTTTCAGCAGGCAGAGGTAA-3' (reverse). The probe specific for MLCK consisted of FAM-5'-TGAAGATGCTGGCTCC-3'-TAMRA. The internal control housekeeping gene GAPDH (glyceraldehyde-3-phosphate dehydrogenase)-specific primer pairs consisted of 5'-CCACCCATGGCAAATTCC-3' (forward), 5'-TGGGATTTCCATTGATGACCAG-3' (reverse). The probe specific for GAPDH consisted of JOE-5'-TGGCACCGTCAAGGCTGAGAACG-3'-TAMRA. All runs were performed according to the following PCR protocol (50°C for 2 min, 95°C for 10 min, 40 cycles for 95°C for 15 s, and 60°C for 1 min). For each sample, real-time PCR was performed in triplicate, and the average threshold cycle was calculated. A standard curve was generated to convert the threshold cycle to copy numbers. Expression of MLCK mRNA was normalized to GAPDH mRNA expression. The average copy number of MLCK mRNA expression in control samples was set to 1.0. The relative expression of MLCK mRNA in treated

samples was determined as a fold increase compared with control samples.

**Transfection of MLCK promoter construct and assessment of promoter activity.** DNA construct of MLCK promoter was transiently transfected into Caco-2 cells by use of transfection reagent Lipofectamine 2000 (Life Technologies) (56). Renilla luciferase vector (pRL-TK, Promega) was cotransfected with each plasmid construct as an internal control. Cells ( $5 \times 10^5$  per filter) were seeded into a six-well Transwell plate and grown to confluence. Caco-2 monolayers were then washed twice with PBS, 1.0 ml of Opti-MEM was added to the apical compartment of each filter, and 1.5 ml was added to the basolateral compartment of each filter. One microgram of plasmid construct and 0.25  $\mu$ g of pRL-TK or 2  $\mu$ l of Lipofectamine 2000 were preincubated in 250  $\mu$ l of Opti-MEM, respectively. After 5 min of incubation, the two solutions were mixed and incubated for another 20 min, and the mixture was added to the apical compartment of each filter. After incubation for 3 h at 37°C, 500  $\mu$ l of DMEM containing 10% FBS was added to both sides of the filter to reach a 2.5% final concentration of FBS. Subsequently, medium was replaced with normal Caco-2 growth medium 16 h after transfection. Specific experiments were carried out 48 h after transfection. At the completion of specific experimental treatments, Caco-2 cells were washed twice with 1 ml of ice-cold PBS followed by the addition of 400  $\mu$ l  $1 \times$  passive lysis buffer, incubated at room temperature for 15 min, scraped and transferred into an Eppendorf tube, and centrifuged for 15 s at 13,000 rpm in a microcentrifuge. Luciferase activity was determined using a dual luciferase assay kit (Promega). Twenty microliters of the supernatant was used for each assay. Luciferase values were determined by Lumat LB 9507 (EG&G Berthold, Oak Ridge, TN). The values of reporter luciferase activities were then divided by that of Renilla luciferase activities to normalize for differences in transfection efficiencies. The average activity value of the control samples was set to 1.0. The luciferase activity of MLCK promoter in treated samples was determined relative to the control samples.

**Determination of mouse intestinal TJ permeability.** The Laboratory Animal Care and Use Committee at the University of New Mexico approved all experimental protocols. Wild-type (WT) mice (of C57BL/6 background) 9 wk of age were obtained from The Jackson Laboratory (Bar Harbor, ME). Generation of MLCK<sup>-/-</sup> mice was described previously (50). The mice were kept two per cage in a temperature-controlled room at 25°C with a 12:12-h light-dark cycle (lights on at 0700). Intestinal permeability in an *in vivo* mouse model system was established using a recycling intestinal perfusion method (12). MMP-9 (10  $\mu$ g/kg) was intraperitoneally injected into the mouse daily for 2 days, after which a 6-cm segment of mouse small intestine was isolated in an anesthetized mouse and cannulated with a small-diameter plastic tube and continuously perfused with 5 ml of Krebs-phosphate saline buffer for a 2-h perfusion period. An external recirculating pump (Econo Pump, Bio-Rad) was used to recirculate the perfusate at a constant flow rate (0.75 ml/min). The body temperature of the mouse was maintained at 37°C with a temperature-controlled warming blanket. Intestinal permeability was assessed by measuring the flux rate of the paracellular probe, Texas Red-labeled dextran (MW 10,000 Da). Water absorption was determined using a nonabsorbable marker, sodium ferrocyanide (cat. no. 39660; Alfa Aesar, Ward Hill, MA) or by measuring the difference between the initial and final volumes of the perfusate.

***In vivo* transfection of MLCK siRNA.** The effect of MLCK siRNA on mouse small intestinal TJ permeability was determined using the perfusion model described previously (23). In these studies, mice were fasted for 24 h before the surgery. With the abdominal cavity open, a 6-cm segment of mouse small intestine was isolated. The transfection solution (0.5 ml), consisting of MLCK siRNA (2.5 nmol) or scramble nontarget siRNA and transfecting agent Lipofectamine (50  $\mu$ l), was injected through a 33-gauge needle into the lumen of the small intestine, and the small intestine was cannulated for 1 h. The small intestine was

placed back into the abdominal cavity, and the abdominal cavity was closed with sutures. MLCK siRNA transfection was performed at *day 0*. After 2 days of MMP-9 (10  $\mu\text{g}/\text{kg}$  body wt ip) treatment, intestinal permeability was measured using the recycling intestinal perfusion method described above. The surgery had no effect on the food intake or body weight of the animals during the experimental period.

**Serum sampling and ELISA method for the quantification of human MMP-9.** Serum samples were collected from 14 healthy (non-IBD) controls and 14 IBD patients (CD = 7; UC = 7). From all individuals written informed consent was obtained, and the study was approved by the University of New Mexico Institutional Review Board, Protocol no. 10-481. A MMP-9 assay ELISA kit (Sigma-Aldrich) based on monoclonal antibodies to human MMP-9 was used to quantify MMP-9 in control and IBD patients' serum, following the manufacturer's instructions.

**Statistical analysis.** Results are expressed as means  $\pm$  SE. Statistical significance of differences between mean values was assessed with Student's *t*-tests for unpaired data (GraphPad Prism 5.00 for Windows, GraphPad Software). All reported significance levels represent two-tailed *P* values. A *P* value of  $\leq 0.05$  was used to indicate statistical significance. All experiments were repeated at least three times to ensure reproducibility.

## RESULTS

MMP-9 is known to be elevated in patients with IBD. To determine the clinically achievable serum concentrations of MMP-9 in patients with IBD, serum MMP-9 levels were measured in healthy volunteers and patients with active CD or UC by using a human MMP-9 ELISA assay. The serum level of MMP-9 was markedly elevated in patients with CD ( $n = 7$ ) and UC ( $n = 7$ ) compared with healthy subjects ( $n = 14$ ) and ranged up to 2,000 ng/ml (Fig. 1A) (Human IRB Protocol no. 10-481). These results suggested that the serum MMP-9 levels can range up to 2,000 ng/ml in IBD patients.

**MMP-9 causes an increase in Caco-2 TJ permeability.** In the following studies, we examined the concentration and time course of MMP-9 effect on intestinal epithelial TJ permeability by measuring transepithelial resistance (TER) and mucosal-to-serosal flux of a paracellular marker inulin (mw = 5,000 g/mol) in filter-grown Caco-2 monolayers (5). MMP-9 caused a concentration (0–1000 ng/ml) and time (0–72 h)-dependent drop in Caco-2 TER (Fig. 2, A and B). MMP-9 caused a

significant drop in Caco-2 TER starting at concentration of  $\sim 300$  ng/ml, and a near-maximum drop in Caco-2 TER occurred  $\sim 400$  ng/ml. Based on the concentration effect, MMP-9 concentration of 400 ng/ml was selected for all of the subsequent experiments. MMP-9 (400 ng/ml) also caused a time-dependent increase in transepithelial flux to paracellular marker inulin (Fig. 2C). The membrane specificity of the effect of MMP-9 on Caco-2 TJ permeability was next determined. MMP-9 (400 ng/ml) was selectively added to the basolateral, apical, or combined apical and basolateral membrane compartments. The apical treatment of MMP-9 did not have significant effect on Caco-2 TER (Fig. 2D). In contrast, the addition of MMP-9 to the basolateral compartment produced a significant drop in Caco-2 TER. The extent of the TER drop was similar whether MMP-9 was added to the basolateral compartment alone or to both basolateral and apical compartments. Together, these findings suggested that MMP-9 presence at the basolateral membrane compartment was both necessary and sufficient for the MMP-9-induced increase in Caco-2 TJ permeability.

**MMP-9 causes an increase in MLCK expression and activity.** Previous studies from our laboratory and others' have shown MLCK to be a key effector protein regulating intestinal epithelial TJ permeability (4, 48). Since the intracellular mechanisms that mediate the MMP-9 effect on intestinal epithelial TJ permeability are unknown, we hypothesized that the TJ effector protein MLCK plays a central role in the MMP-9 effect. In the following studies, the effect of MMP-9 on Caco-2 MLCK expression was determined. MMP-9 (400 ng/ml) caused a time-dependent increase in MLCK protein expression in Caco-2 cells, as determined by Western blot analysis (Fig. 3A). The effect of MMP-9 on MLCK kinase activity was next determined by *in vitro* kinase activity measurement. MMP-9 caused a time-dependent increase in MLCK kinase activity starting at 24 h (Fig. 3B), correlating with the time course of the increase in MLCK expression (Fig. 3A). MMP-9 also caused a time-dependent increase in phosphorylated MLC in Caco-2 monolayers, similar to *in vitro* kinase studies. The effect of pharmacological MLCK inhibitor ML-7 on the MMP-9-induced increase in Caco-2 TJ permeability was next determined. ML-7, at a dose known to selectively inhibit Caco-2 MLCK activity (10  $\mu\text{M}$ ) (4), significantly inhibited the MMP-9-induced increase in mucosal-to-serosal flux of inulin (Fig. 3D). To further validate the involvement of MLCK in the MMP-9-induced increase in Caco-2 TJ permeability, MLCK was knocked down by transfecting filter-grown Caco-2 monolayers with MLCK siRNA. The MLCK siRNA transfection caused a near-complete depletion of MLCK protein expression (Fig. 3E) and significantly attenuated the MMP-9-induced increase in inulin flux (Fig. 3F), confirming that the MMP-9-induced increase in Caco-2 TJ permeability was mediated in part by an increase in MLCK expression.

**MMP-9 activates the p38 kinase signaling pathway.** Previous studies have suggested that mitogen-activated protein kinase signaling pathways, including extracellular signal regulated kinase (ERK)1/2, p38 kinase, and c-Jun NH<sub>2</sub>-kinase (JNK) may be activated by MMP-9 and could potentially play a role in mediating inflammatory and biological responses (2, 15, 51). To identify the specific signaling kinase pathway involved in MMP-9 modulation of intestinal TJ barrier, we examined the involvement of ERK1/2, p38 kinase, and JNK. MMP-9 (400

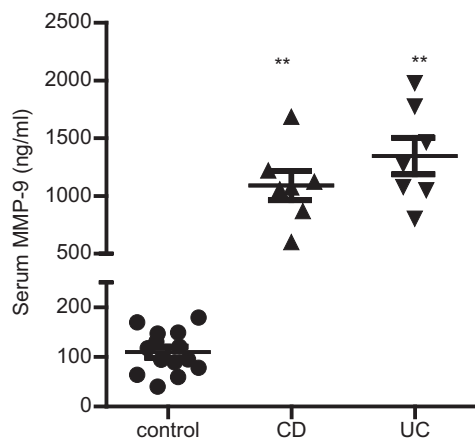
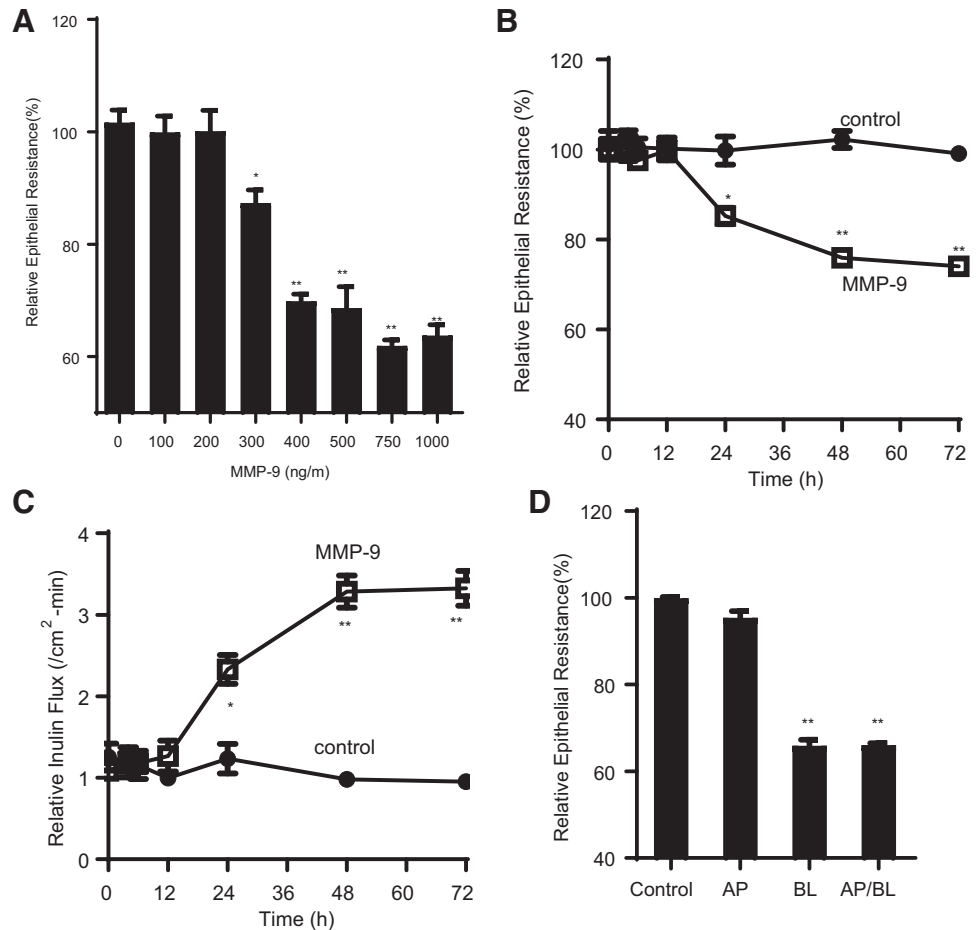


Fig. 1. Matrix metalloproteinase-9 (MMP-9) serum levels (ng/ml) in inflammatory bowel disease (IBD) patients [ulcerative colitis (UC),  $n = 7$ ; Crohn's disease (CD),  $n = 7$ ] compared with healthy controls;  $n = 14$ . \*\* $P < 0.001$ .

Fig. 2. Effect of matrix metalloproteinase-9 (MMP-9) on Caco-2 tight junction (TJ) permeability. **A:** MMP-9 caused a concentration-dependent drop in Caco-2 transepithelial electrical resistance (TER);  $n = 4$ .  $*P < 0.01$  vs. control,  $**P < 0.001$  vs. control. **B:** MMP-9 (400 ng/ml) caused a time-dependent drop in Caco-2 TER;  $n = 4$ .  $*P < 0.01$  vs. control,  $**P < 0.001$  vs. control. **C:** MMP-9 (400 ng/ml) caused a time-dependent increase in inulin flux;  $n = 4$ .  $*P < 0.01$  vs. control,  $**P < 0.001$  vs. control. **D:** membrane specificity of the effect of MMP-9 on Caco-2 TER. MMP-9 was added to apical (AP), basolateral (BL), or combined apical + basolateral compartments for the 48-h experimental period. Addition of MMP-9 to the basolateral or combined basolateral + apical compartments produced a significant drop in Caco-2 TER;  $n = 4$ .  $**P < 0.001$ .



ng/ml) caused a rapid, time-dependent increase in p38 kinase phosphorylation at Tyr<sup>182</sup> (53) (Fig. 4A) starting at ~20 min, consistent with p38 kinase activation. However, MMP-9 did not have any effect on ERK1/2 or JNK phosphorylation (Fig. 4A). To confirm the increase in p38 kinase activity, the *in vitro* kinase activity of p38 kinase was also determined using ATF-2 as the substrate (2). MMP-9 caused a time-dependent increase in p38 kinase activity (Fig. 4B) in Caco-2 monolayers. The p38 kinase pharmacological inhibitor, SB-203580 (10  $\mu$ M), inhibited the MMP-9-induced increase in p38 phosphorylation, kinase activity, and also the increase in inulin flux (Fig. 4, C–E). These data suggested that p38 kinase activation was required for the MMP-9-induced increase in Caco-2 TJ permeability. Since the above studies suggested that the MMP-9-induced increase in Caco-2 TJ permeability was due, in part, to an increase in MLCK protein/activity, the possible regulatory role of p38 kinase pathway on MLCK expression/activity was also examined. The p38 kinase inhibitor SB-203580 prevented the MMP-9 induced increase in MLCK activity and MLCK protein expression (Fig. 5, A and B), suggesting that the p38 kinase pathway signals the MMP-9 modulation of MLCK protein expression and MLCK activity. To further validate the requirement of p38 kinase for MLCK expression, p38 kinase expression was knocked down by p38 kinase siRNA. The Caco-2 transfection of p38 kinase siRNA caused a depletion of p38 kinase in filter-grown Caco-2 monolayers (Fig. 5C). The siRNA knockdown of p38 kinase inhibited the MMP-9-in-

duced increase in MLCK activity and protein expression (Fig. 5, C and D) and the increase in Caco-2 TJ permeability (Fig. 5E), confirming the regulatory role of p38 kinase pathway in the MMP-9-induced increase in MLCK expression/activity and Caco-2 TJ permeability.

**MMP-9 targets the MLCK gene.** The above studies suggested that the MMP-9 induced increase in Caco-2 TJ permeability was regulated in part by an increase in the effector protein MLCK. In the following studies, we tested the hypothesis that MMP-9 targets the MLCK gene activation. The MMP-9 (400 ng/ml) effect on MLCK promoter activity and mRNA expression was examined. In these studies, Caco-2 cells were transfected with the plasmid vector encoding the MLCK promoter region (2,091 bp) and MLCK promoter activity was determined by luciferase assay as previously described (4). MMP-9 caused an increase in MLCK promoter activity in Caco-2 monolayers (Fig. 6A). MMP-9 also caused a time-dependent increase in MLCK mRNA levels, as assayed by real-time PCR (Fig. 6B). The possible involvement of p38 kinase pathway in signaling MMP-9 activation of MLCK gene was next determined. As described above, MMP-9 causes the activation of p38 kinase. The effect of p38 kinase inhibitor and siRNA induced knockdown on MMP-9 induced activation of MLCK gene activity was examined. Pharmacological inhibition of p38 kinase activity by SB-203580 or siRNA induced knockdown of p38 kinase prevented the MMP-9 induced increase in MLCK promoter activity and mRNA transcription

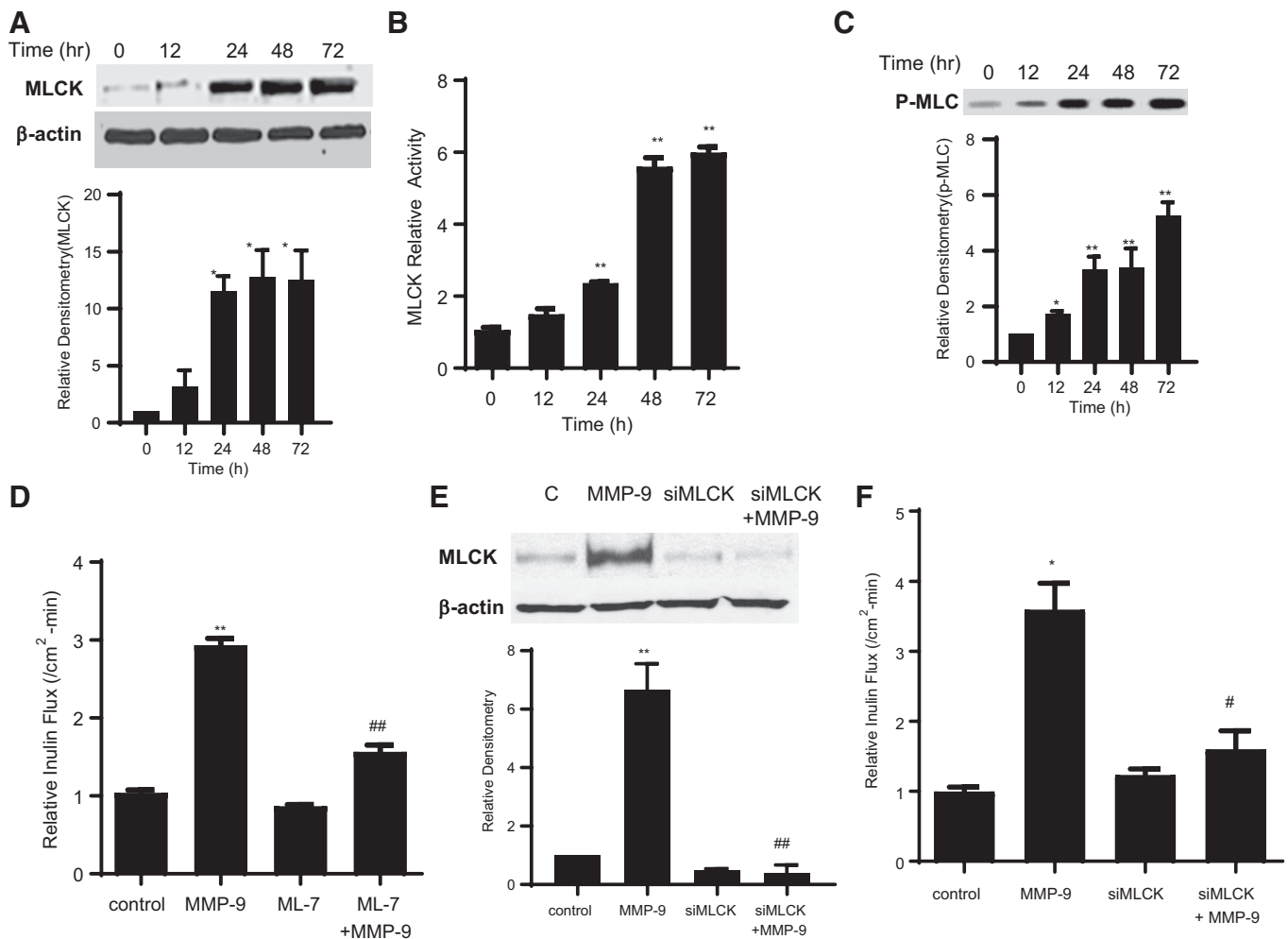


Fig. 3. Effect of matrix metalloproteinase-9 (MMP-9) on myosin light-chain kinase (MLCK) activity and expression. MMP-9 (400 ng/ml) caused a time-dependent increase in MLCK protein expression (A), and an increase in MLCK in vitro kinase activity (B);  $n = 4$ ,  $**P < 0.001$  vs. control; and an increase in phosphorylated (p)-MLC (C), as assessed by Western blot analysis. D: pretreatment with ML-7 (1 h before MMP-9 treatment) prevented the MMP-9 induced increase in inulin flux (48-h experimental period;  $n = 4$ ,  $**P < 0.001$  vs. control;  $###P < 0.001$  vs. MMP-9 treatment). E: MLCK small interfering (si)RNA transfection resulted in near-complete depletion in MLCK protein expression, as determined by Western blot analysis and prevented the MMP-9-induced increase in MLCK protein expression. siRNA transfection was performed 24 h before MMP-9 treatment (48-h experimental period). F: MLCK siRNA transfection prevented the MMP-9-induced increase in Caco-2 inulin flux (48-h experimental period),  $n = 4$ ,  $**P < 0.001$  vs. control;  $#P < 0.01$  vs. MMP-9 treatment.

(Fig. 6, C–F), indicating that p38 kinase signaling pathway mediated the MMP-9 activation of MLCK gene.

**MMP-9 causes an increase in mouse intestinal permeability in vivo.** Although the above-mentioned studies show that MMP-9 causes an increase in Caco-2 intestinal epithelial TJ permeability, the effects of MMP-9 on intestinal permeability in live animals remain unknown. In the following studies, the effect of MMP-9 on mouse intestinal permeability in live mice was determined in vivo using a recycling intestinal perfusion method (3). MMP-9 (10  $\mu$ g) was administered by intraperitoneal injection as previously described. The mouse intestinal permeability was then assessed by measuring the luminal-to-serosal flux rate of the paracellular probe Texas Red-labeled dextran (MW = 10,000 g/mol), by measuring the disappearance of dextran from the perfusate solution. Intraperitoneal MMP-9 injection resulted in a time-dependent increase in mouse intestinal permeability in vivo starting at the 24-h time point (Fig. 7A).

We next determined the effect of MMP-9 (10  $\mu$ g) on MLCK protein expression in mice intestinal tissue. The intraperitoneal

injection of MMP-9 resulted in a marked increase in MLCK protein expression in the intestinal tissue, which correlated with the MMP-9-induced increase in mouse intestinal TJ permeability (Fig. 7B). The MMP-9 effect on mouse MLCK protein expression did not occur at earlier time points of treatment (6 and 12 h) but peaked at 24 and 48 h of treatment. We also examined whether MMP-9 preferentially activated p38 kinase in intestinal tissue. MMP-9 caused an activation of p38 kinase at the 2-h time point, as evidenced by p38 phosphorylation (Fig. 7C). MMP-9 did not cause an increase in phosphorylation of ERK1/2 or JNK (data not shown). The requirement of MLCK in the MMP-9-induced increase in mouse intestinal permeability was determined by siRNA-induced knockdown of mouse intestinal MLCK in vivo. In brief, a 6-cm segment of small intestinal mucosal surface was isolated and the mucosal surface exposed to a short pulse (1 h) of transfecting solution containing MLCK siRNA. The effect of MLCK siRNA transfection of intestinal epithelial cells on mouse intestinal permeability was determined following MMP-9 treatment. In vivo MLCK siRNA transfection of mouse enterocytes prevented the MMP-9 in-

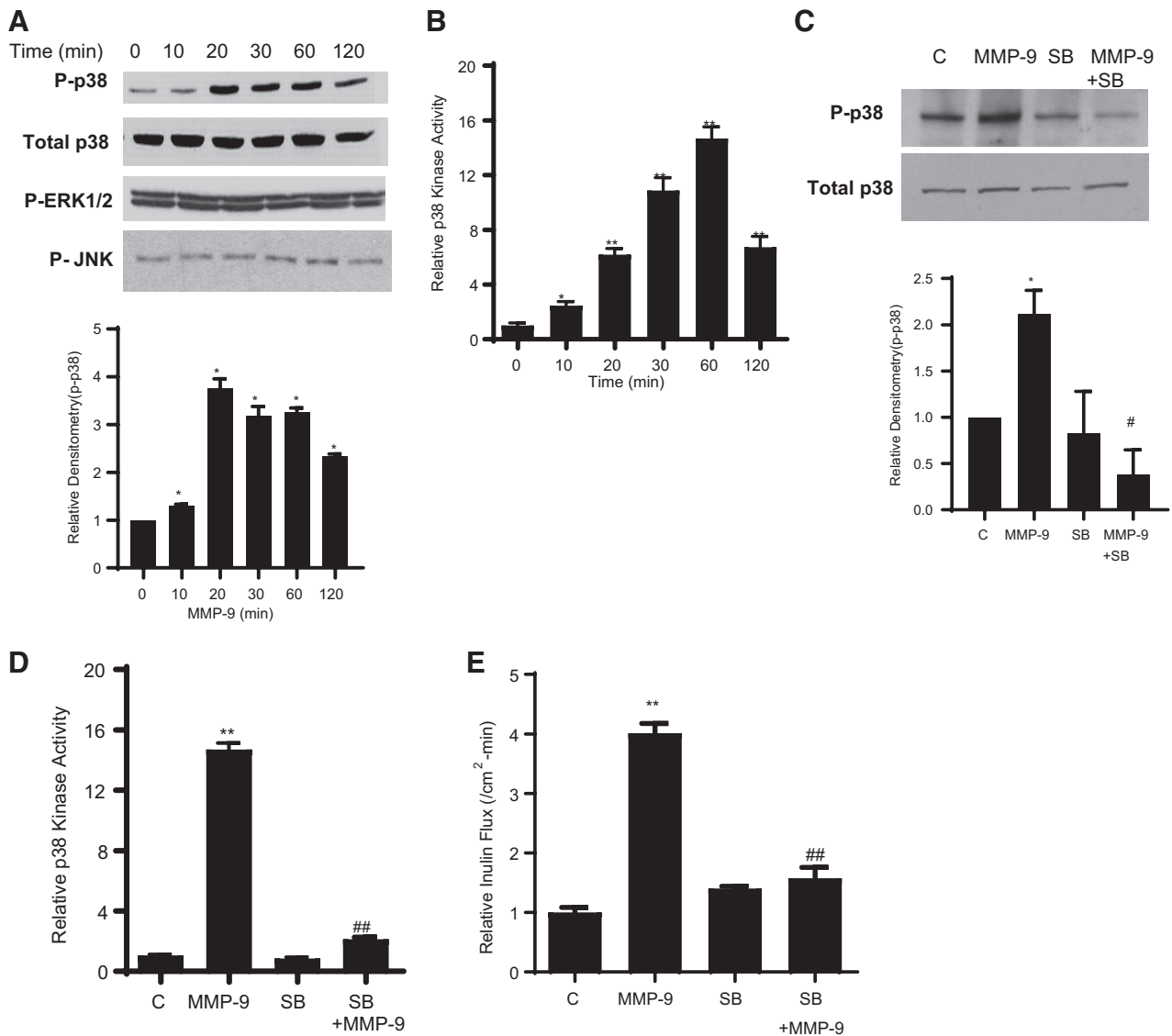


Fig. 4. Effect of matrix metalloproteinase-9 (MMP-9) on p38 kinase activity. **A:** MMP-9 caused a rapid time-dependent increase in phosphorylation of p38 kinase at Tyr<sup>182</sup> as assessed by Western blot analysis, but did not affect extracellular signal-regulated kinase (ERK)1/2 or c-Jun NH<sub>2</sub>-kinase (JNK) phosphorylation. **B:** MMP-9 caused a time-dependent increase in *in vitro* p38 kinase activity assessed by phosphorylation of activating transcription factor 2 (ATF-2) as the substrate;  $n = 4$ . \* $P < 0.01$  vs. control (C), \*\* $P < 0.001$  vs. control. Pretreatment with p38 kinase inhibitor SB-203580 (SB; 10  $\mu$ M), 1 h before MMP-9 treatment, prevented the MMP-9-induced increase in p38 kinase phosphorylation (1-h experimental period; \* $P < 0.01$  vs. control, # $P < 0.01$  vs. MMP-9 treatment; **C**) and inhibited the MMP-9 induced increase in p38 kinase activity (1-h experimental period; **D**);  $n = 3$ . \*\* $P < 0.001$  vs. control; ## $P < 0.001$  vs. MMP-9 treatment. **E:** SB-203580 pretreatment, 1 h before MMP-9 treatment, prevented the MMP-9 induced increase in inulin flux (48-h experimental period;  $n = 4$ . \*\* $P < 0.001$  vs. control; ## $P < 0.001$  vs. MMP-9 treatment).

duced increase in MLCK protein expression (Fig. 7D) and inhibited the MMP-9-induced increase in mouse intestinal permeability (Fig. 7E). The effect of MMP-9 on mouse intestinal permeability was also next examined in MLCK<sup>-/-</sup> mice. MMP-9 treatment did not cause an increase in intestinal permeability in MLCK knockout mice (Fig. 7F). Collectively, these data suggested that MMP-9 causes an increase in mouse intestinal MLCK expression and that the increase in MLCK was required for the MMP-9-induced increase in mouse intestinal permeability.

## DISCUSSION

MMP-9 is the main metalloproteinase implicated in the development of IBD (21, 46). Studies in MMP-9-deficient

mice demonstrated that MMP-9 is an important pathogenic factor mediating intestinal inflammation (46). Studies in cell lines and animal models indicated that the development of intestinal inflammation was attenuated by the application of metalloproteinase inhibitors (21, 30). The severity of DSS colitis was also significantly decreased in MMP-9-deficient mice. The loss of body weight, clinical disease activity score, and colonic histological score of inflammation were attenuated in MMP-9-deficient mice treated with DSS compared with the control mice (40). As shown in Fig. 1 and in studies from other laboratories, MMP-9 is elevated in intestinal tissue and serum of patients with IBD (19, 29). Defective intestinal TJ barrier is an important pathogenic factor contributing to the development of intestinal inflammation in IBD and other inflammatory

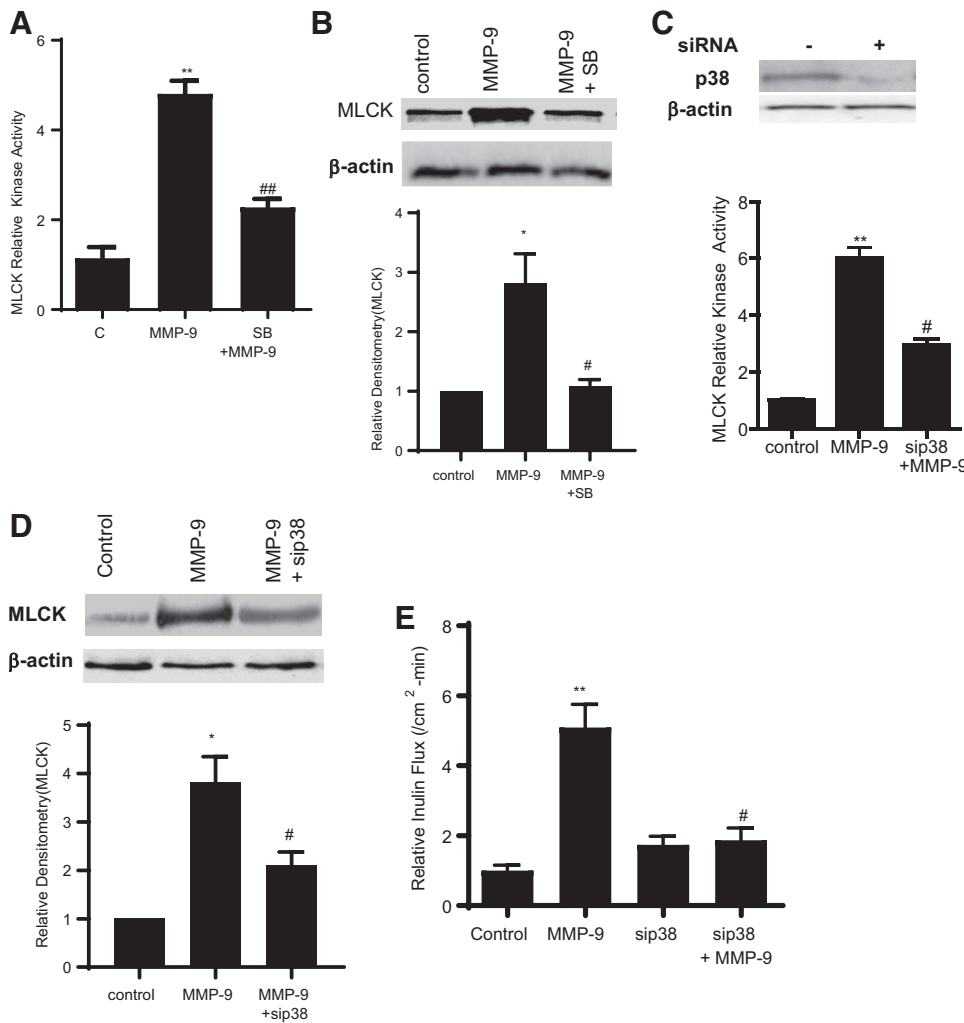


Fig. 5. Involvement of p38 kinase signaling pathway in matrix metalloproteinase-9 (MMP-9)-induced activation of myosin light-chain kinase (MLCK) in Caco-2 monolayers. **A**: pretreatment with p38 kinase inhibitor SB-203580 (10  $\mu$ M), 1 h before MMP-9 treatment, prevented the MMP-9-induced increase in MLCK kinase activity (48-h experimental period;  $n = 4$ . \*\* $P < 0.001$  vs. control; ## $P < 0.001$  vs. MMP-9 treatment. **B**: SB-203580 prevented the MMP-9-induced increase in MLCK protein expression as assessed by Western blot analysis (48-h experimental period;  $n = 3$ . **C**: small interfering (si)RNA-induced knockdown of p38 kinase resulted in near-complete depletion of p38 kinase expression as assessed by Western blot analysis ( $n = 3$ ) and prevented the MMP-9-induced increase in MLCK kinase activity;  $n = 4$ . \*\* $P < 0.001$  vs. control; # $P < 0.01$  vs. MMP-9 treatment. siRNA transfection was performed 24 h before MMP-9 treatment (48-h experimental period). **D**: siRNA-induced knockdown of p38 kinase significantly inhibited the MMP-9-induced increase in MLCK protein expression (48-h experimental period;  $n = 3$ . **E**: siRNA-induced knockdown of p38 kinase also prevented the MMP-9-induced increase in inulin flux (48-h experimental period;  $n = 4$ . \*\* $P < 0.001$  vs. control; # $P < 0.01$  vs. MMP-9 treatment.

disorders (24, 45). Proinflammatory mediators, including tumor necrosis factor- $\alpha$  (TNF $\alpha$ ), interleukin (IL)-1 $\beta$ , and interferon- $\gamma$  (IFN $\gamma$ ), have been shown to cause an increase in intestinal TJ permeability. However, the role of metalloproteinases in the modulation of intestinal TJ barrier function remains unclear. The focus of the present study was to investigate the effect of the proinflammatory metalloproteinase MMP-9 in the modulation of intestinal epithelial TJ permeability. Herein, we show that the clinically relevant concentrations (0–1,000 ng/ml) of MMP-9 cause a progressive increase in Caco-2 intestinal epithelial TJ permeability and mouse intestinal permeability and that the increase in TJ permeability was mediated in part by an increase in the expression of TJ effector protein MLCK. Our studies in Caco-2 monolayers showed that MMP-9 treatment at the apical compartment did not cause change in Caco-2 TJ permeability, whereas MMP-9 treatment to both the basolateral compartment and the apical compartment caused an increase in Caco-2 TJ permeability. Moreover, MMP-9 treatment at both the apical and basolateral compartments did not cause a greater increase in Caco-2 TJ permeability than addition to the basolateral membrane alone, suggesting that the MMP-9 induced increase in Caco-2 TJ permeability was due to MMP-9 effect on the basolateral membrane. Consistent with the *in vitro* data, treatment with MMP-9 intraperitoneally caused an increase in mouse intestinal

permeability *in vivo*, confirming that the *in vivo* effect of MMP-9 was also mediated by its presence in the interstitial fluid or on the basolateral membrane surface. Previous clinical studies had demonstrated a correlation between an increase in MMP-9 levels and an increase in disease activity in IBD (19, 29). Herein, we show that physiologically and clinically relevant concentrations of MMP-9 cause an increase in intestinal epithelial TJ permeability *in vitro* and *in vivo* when present in the basolateral membrane compartment. These data suggest that relatively low levels of MMP-9 in the interstitial fluid, which are readily achievable during physiological stresses or in intestinal permeability disorders, lead to an increase in intestinal permeability. Previous studies have shown that MMP-9 induces the activation of basolateral membrane-expressed receptors such as epidermal growth factor receptor (EGFR) in COS-1 monkey kidney epithelial cells. Dufour et al. (18) found that MMP-9-enhanced, protease-independent cell migration involves the coordination of pro-MMP-9 domain homodimerization and CD44 heterodimerization, leading to EGFR phosphorylation and subsequent activation of the MAP kinase signaling cascade. Other studies, by Abdulkhalek et al. (1), using mouse macrophages and dendritic cells demonstrated that MMP-9 colocalizes with Toll-like receptor 4 (TLR-4) on the cell surface and potentiates the LPS-activation of TLR-4 and the induction of the intracel-



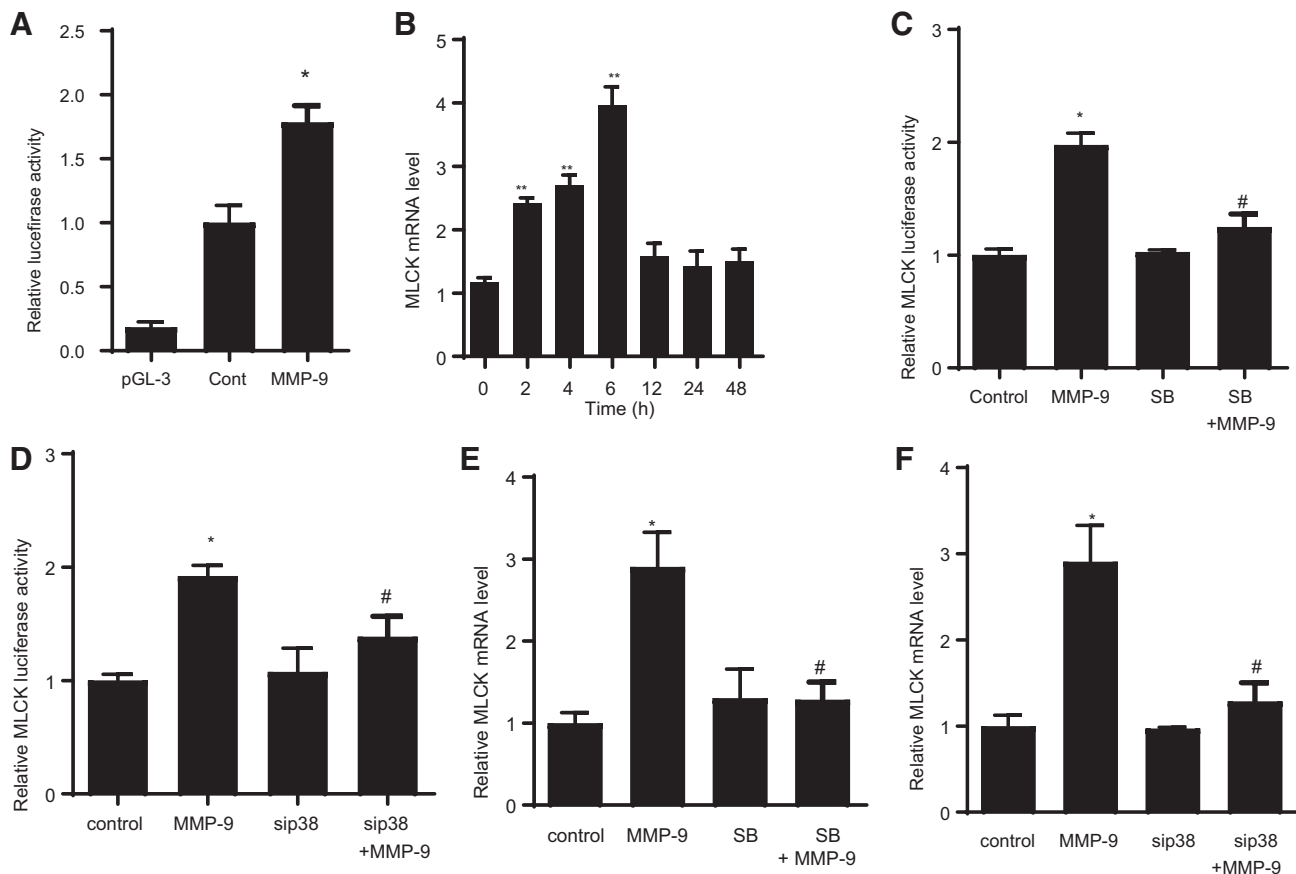


Fig. 6. Effect of matrix metalloproteinase-9 (MMP-9) on myosin light-chain kinase (MLCK) gene activity. **A:** MMP-9 caused an increase in MLCK promoter activity of the full-length MLCK promoter region (2,091 bp) in Caco-2 monolayers (4-h experimental period). pGL-3 basic vector containing the MLCK promoter region was transfected into filter-grown Caco-2 cells. Caco-2 cells were treated with MMP-9 (400 ng/ml) for 4 h. MLCK promoter activity was determined by luciferase assay and expressed as relative luciferase activity;  $n = 8$ . \* $P < 0.01$  vs. control. **B:** MMP-9 (400 ng/ml) caused a time-dependent increase in MLCK mRNA levels as assayed by real-time PCR, peaking at 6 h posttreatment and returning to basal levels at 12 h ( $n = 6$ ). \*\* $P < 0.001$  vs. control. Pretreatment with p38 kinase inhibitor SB-203580 (SB; 10  $\mu$ M), 1 h before MMP-9 treatment (**C**) and small interfering (si)RNA-induced knockdown of p38 kinase expression (**D**) attenuated the MMP-9 induced increase in MLCK promoter activity as assessed by luciferase activity. Caco-2 monolayers were cotransfected with siRNA p38 kinase for 48 h before MMP-9 treatment (4-h experimental period;  $n = 8$ ). \* $P < 0.01$  vs. control, \*\* $P < 0.0001$  vs. MMP-9 treatment. Pretreatment with p38 kinase inhibitor SB-203580 (10  $\mu$ M; **E**), and siRNA-induced knockdown of p38 kinase (**F**) prevented the MMP-9-induced increase in Caco-2 MLCK mRNA levels;  $n = 5$ . \* $P < 0.01$  vs. control; # $P < 0.01$  vs. MMP-9 treatment (6-h experimental period).

lular signaling pathway, including activation of the NF- $\kappa$ B pathway. Inhibition of MMP-9 by short hairpin RNA (*shRNA*) and small interfering RNA (siRNA) prevented the LPS-induced activation of TLR-4 and activation of NF- $\kappa$ B in macrophages and dendritic cells. Taken together, these studies show that MMP-9 induces intracellular signaling pathways by activating distinct membrane receptors. Identifying the specific membrane receptors that mediate the MMP-9-induced increase in intestinal TJ permeability could be important in developing future therapeutic strategies in IBD.

Previous studies have shown that MMP-9 induces the activation of MAP kinases, including ERK1/2, p38 kinase, and JNK (16, 42–44, 57). To determine the signaling pathway involved in the TJ barrier regulation, we studied the possible involvement of the three MAP kinases. Our studies indicated that MMP-9 activated p38 kinase but not ERK1/2 or JNK. The p38 kinase was rapidly activated by MMP-9 within 20–30 min and preceded the MMP-9-induced increase in Caco-2 TJ permeability; and inhibition of p38 kinase activity prevented the MLCK gene activation, the increase in MLCK expression, and the increase in Caco-2 TJ permeability. Thus, our studies

showed that the p38 kinase signaling pathway mediated the increase in MLCK gene activity and Caco-2 TJ permeability.

Previous studies from our laboratory and others' have shown the integral role of MLCK in both physiological and pathological regulation of intestinal epithelial TJ permeability (4, 13, 20, 34, 47). MLCK is expressed in the intestinal epithelial cells and MLCK isoform MLCK1 is concentrated near the perijunctional actomyosin ring. The increase in enterocyte MLCK activity either by an increase in MLCK expression or by an increase in MLCK specific activity leads to an enzymatic phosphorylation of MLC and subsequent stepwise amplification cascade of intracellular processes, leading to the activation of  $Mg^{2+}$ -myosin ATPase and energy-dependent contraction of perijunctional actin/myosin filaments, which, in turn, generate mechanical tension and energy-dependent retraction of the TJ complex and the plasma membrane, culminating in the separation of the junctional complexes and the opening of the paracellular pathways (35, 37). The central importance of MLCK in the regulation of the intestinal TJ barrier is firmly established (4, 12, 34). MLCK is an important regulator of the intestinal TJ barrier during inflammatory conditions, and pro-

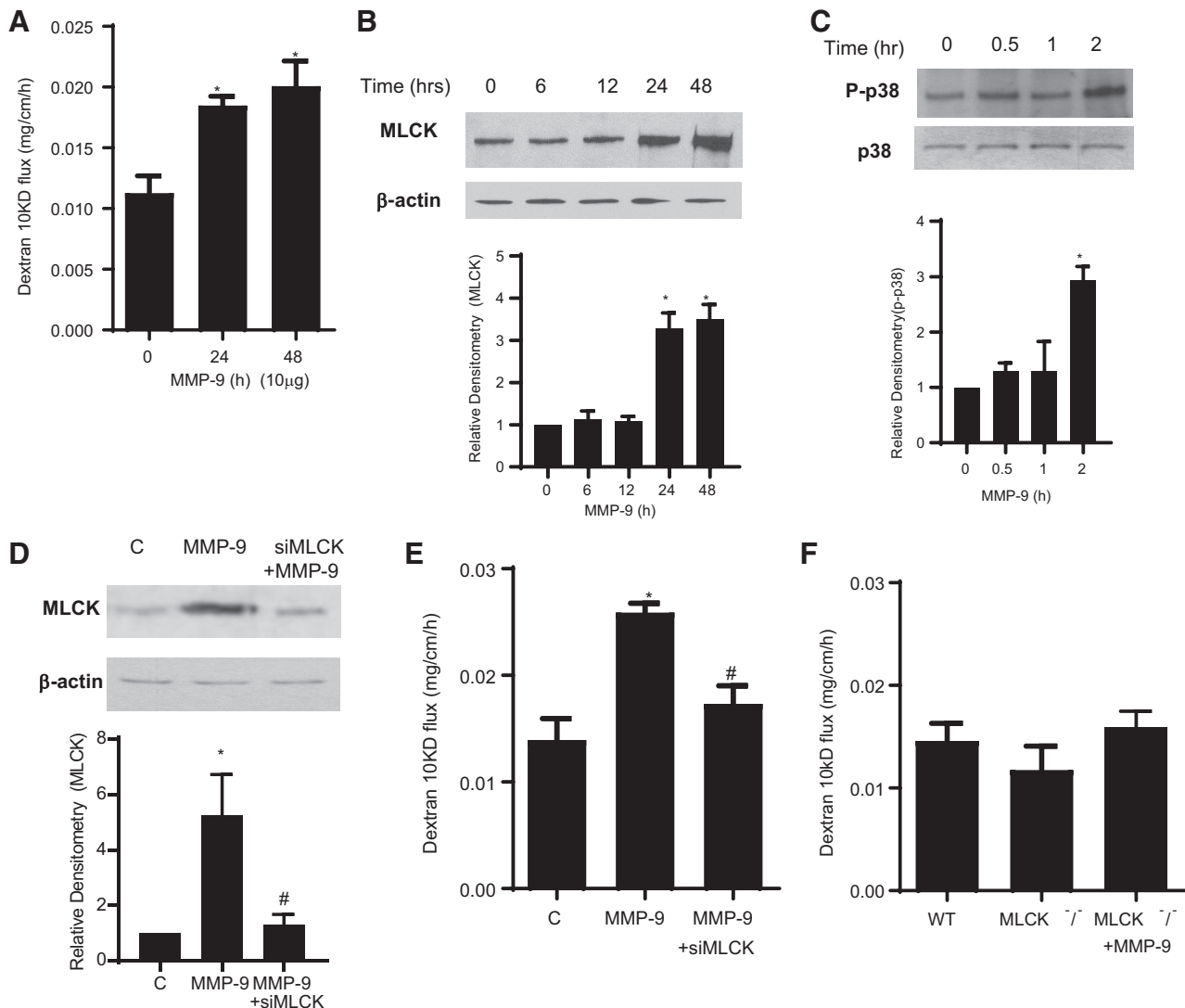


Fig. 7. Effect of matrix metalloproteinase-9 (MMP-9) on mouse intestinal permeability in vivo. **A:** MMP-9 (10  $\mu$ g ip) injection caused an increase in mouse small intestinal permeability as assessed by dextran (10 kDa) flux in mouse small intestine of wild-type (WT) mice;  $n = 12$  control WT mice,  $n = 4$  treated WT mice.  $*P < 0.01$  vs. control. **B:** MMP-9 treatment resulted in an increase in intestinal tissue myosin light-chain kinase (MLCK) protein expression starting at 24 h of treatment as assessed by Western blot analysis. **C:** MMP-9 caused an increase in phosphorylation of p38 kinase at Tyr<sup>182</sup> after 2-h experimental period as assessed by Western blot analysis. **D:** In vivo small interfering (si)RNA-induced knockdown of mouse enterocyte MLCK prevented the MMP-9-induced increase in MLCK protein expression (24-h experimental period) and attenuated the MMP-9-induced increase in mouse intestinal permeability (24-h experimental period);  $n = 12$  control wild-type (WT) mice,  $n = 4$  treated WT mice.  $*P < 0.01$  vs. control;  $\#P < 0.01$  vs. MMP-9 treatment. **E:** MMP-9 did not cause an increase in mouse intestinal permeability in MLCK-deficient (MLCK<sup>-/-</sup>) mice (24-h experimental period);  $n = 12$  control WT mice,  $n = 7$  (control MLCK<sup>-/-</sup> mice,  $n = 4$  treated MLCK<sup>-/-</sup> mice).

inflammatory cytokines, including TNF $\alpha$  and IL-1 $\beta$ , target the MLCK gene activation to drive the increase in intestinal TJ permeability. Moreover, targeting MLCK expression or activity with siRNA or pharmacological inhibitors of MLCK has been shown to be effective in preventing or attenuating intestinal inflammation in a number of animal models of IBD (2, 12, 40, 58), highlighting the importance of preserving the intestinal TJ barrier as a therapeutic approach to prevent or treat intestinal inflammation.

It should be noted that in our studies MMP-9 did not affect the TJ protein expression of claudin-1, claudin-2, zonula occludens-1, or another junctional protein expression, E-cadherin, but caused a decrease in occludin expression starting at the 48-h experimental period (data not shown), suggesting that

the decrease in occludin protein expression may also be a contributing factor in the MMP-9-induced increase in Caco-2 TJ permeability. In future studies, we intend to study the role of occludin depletion as a contributing factor to the MMP-9-induced increase in TJ permeability. The studies herein show also that the MMP-9-induced increase in Caco-2 TJ permeability was dependent on the increase in MLCK gene activity and protein expression. The MMP-9-induced increase in Caco-2 TJ permeability correlated with the increase in MLCK expression/activity, and the inhibition of MLCK activity or MLCK expression inhibited the increase in Caco-2 TJ permeability. The MLCK gene activity studies also showed that MMP-9 caused an increase in MLCK promoter activity and mRNA transcription, confirming that the MMP-9 increase in

MLCK protein expression was dependent on MLCK gene activation. Additionally, our MLCK gene regulation studies also suggested that the p38 kinase pathway mediated the MMP-9 activation of MLCK gene. Taken together, our studies showed that the MMP-9-induced increase in Caco-2 TJ permeability was regulated by p38 kinase pathway activation of the MLCK gene. In future studies, we aim to investigate the transcription factors and the molecular determinants that mediate MMP-9-induced MLCK gene activation.

In the present study, we also examined the possible in vivo effects of MMP-9 on mouse intestinal permeability by small intestinal recycling perfusion. MMP-9 caused an increase in mouse intestinal permeability to paracellular marker dextran (10 kDa). The increase in mouse intestinal permeability was accompanied by an increase in intestinal tissue expression of MLCK; and mouse intestinal enterocyte-specific silencing of MLCK by MLCK siRNA prevented the MMP-9-induced increase in mouse intestinal permeability. Additionally, the MMP-9-induced increase in mouse intestinal permeability was also inhibited in MLCK knockout mice. Thus, our mouse intestinal perfusion studies showed that MMP-9 causes an increase in mouse intestinal permeability and that the increase in intestinal permeability required an increase in MLCK expression. The importance of MLCK in the inflammation-associated increase in mouse intestinal permeability has been well demonstrated. A number of studies have demonstrated that in animal models of IBD the increase in mouse intestinal permeability and intestinal inflammation was associated with an increase in intestinal MLCK expression, and inhibition of MLCK expression or MLCK activity inhibited the increase in intestinal permeability and the subsequent development of intestinal inflammation (8, 14, 20). In mouse models of DSS-induced colitis and T cell transfer-induced colitis, the alteration in intestinal permeability preceded the development of intestinal inflammation, and inhibitors of MLCK activity prevented the increase in intestinal permeability and the development of intestinal inflammation (7, 20, 40). Similarly, patients with Crohn's disease and ulcerative colitis have a marked increase in MLCK expression, which is also correlated with the disease activity (31). In this regard, MLCK inhibitors are being targeted as therapy for IBD.

In conclusion, our data show that MMP-9 at clinically achievable concentrations causes an increase in Caco-2 intestinal epithelial TJ permeability. The MMP-9-induced increase in Caco-2 TJ permeability was mediated by p38 kinase signaling pathway activation of MLCK gene and the subsequent increase in MLCK transcription and translation. MMP-9 also caused an increase in mouse intestinal permeability in an MLCK-dependent manner. Thus, our studies show for the first time that MMP-9 has a direct disruptive effect on the intestinal epithelial TJ barrier function and provides new insight into the potential mechanisms by which MMP-9 contributes to the intestinal inflammation.

#### GRANTS

This research project was supported by a Career Development Award from the Crohn's and Colitis Foundation of America (to R. Al-Sadi) and National Institute of Diabetes and Digestive and Kidney Diseases Grant RO1 DK-64165-01 (to T. Y. Ma).

#### DISCLOSURES

No conflicts of interest, financial or otherwise, are declared by the authors.

#### AUTHOR CONTRIBUTIONS

R.A.-S. and T.Y.M. conceived and designed research; R.A.-S., M.Y., M.R., S.G., K.D., and M.H. performed experiments; R.A.-S., M.Y., M.R., S.G., K.D., M.D.W., and T.Y.M. analyzed data; R.A.-S., M.Y., and T.Y.M. interpreted results of experiments; R.A.-S., M.Y., M.R., and S.G. prepared figures; R.A.-S. drafted manuscript; R.A.-S. and T.Y.M. edited and revised manuscript; R.A.-S. and T.Y.M. approved final version of manuscript.

#### REFERENCES

1. **Abdulkhalek S, Amith SR, Franchuk SL, Jayanth P, Guo M, Finlay T, Gilmour A, Guzzo C, Gee K, Beyaert R, Szwczuk MR.** Neu1 sialidase and matrix metalloproteinase-9 cross-talk is essential for Toll-like receptor activation and cellular signaling. *J Biol Chem* 286: 36532–36549, 2011. doi:10.1074/jbc.M111.237578.
2. **Al-Sadi R, Guo S, Ye D, Dokladny K, Alhmod T, Ereifej L, Said HM, Ma TY.** Mechanism of IL-1 $\beta$  modulation of intestinal epithelial barrier involves p38 kinase and activating transcription factor-2 activation. *J Immunol* 190: 6596–6606, 2013. doi:10.4049/jimmunol.1201876.
3. **Al-Sadi R, Guo S, Ye D, Ma TY.** TNF- $\alpha$  modulation of intestinal epithelial tight junction barrier is regulated by ERK1/2 activation of Elk-1. *Am J Pathol* 183: 1871–1884, 2013. doi:10.1016/j.ajpath.2013.09.001.
4. **Al-Sadi R, Ye D, Dokladny K, Ma TY.** Mechanism of IL-1 $\beta$ -induced increase in intestinal epithelial tight junction permeability. *J Immunol* 180: 5653–5661, 2008. doi:10.4049/jimmunol.180.8.5653.
5. **Al-Sadi RM, Ma TY.** IL-1 $\beta$  causes an increase in intestinal epithelial tight junction permeability. *J Immunol* 178: 4641–4649, 2007. doi:10.4049/jimmunol.178.7.4641.
6. **Arrieta MC, Madsen K, Doyle J, Meddings J.** Reducing small intestinal permeability attenuates colitis in the IL10 gene-deficient mouse. *Gut* 58: 41–48, 2009. doi:10.1136/gut.2008.150888.
7. **Bertuccini L, Costanzo M, Iosi F, Tinari A, Terruzzi F, Stronati L, Aloï M, Cucchiara S, Superti F.** Lactoferrin prevents invasion and inflammatory response following *E. coli* strain LF82 infection in experimental model of Crohn's disease. *Dig Liver Dis* 46: 496–504, 2014. doi:10.1016/j.dld.2014.02.009.
8. **Blair SA, Kane SV, Clayburgh DR, Turner JR.** Epithelial myosin light chain kinase expression and activity are upregulated in inflammatory bowel disease. *Lab Invest* 86: 191–201, 2006. doi:10.1038/labinvest.3700373.
9. **Brinckerhoff CE, Matrisian LM.** Matrix metalloproteinases: a tail of a frog that became a prince. *Nat Rev Mol Cell Biol* 3: 207–214, 2002. doi:10.1038/nrm763.
10. **Castaneda FE, Walia B, Vijay-Kumar M, Patel NR, Roser S, Kolachala VL, Rojas M, Wang L, Oprea G, Garg P, Gewirtz AT, Roman J, Merlin D, Sitaraman SV.** Targeted deletion of metalloproteinase 9 attenuates experimental colitis in mice: central role of epithelial-derived MMP. *Gastroenterology* 129: 1991–2008, 2005. doi:10.1053/j.gastro.2005.09.017.
11. **Clayburgh DR, Barrett TA, Tang Y, Meddings JB, Van Eldik LJ, Watterson DM, Clarke LL, Mrsny RJ, Turner JR.** Epithelial myosin light chain kinase-dependent barrier dysfunction mediates T cell activation-induced diarrhea in vivo. *J Clin Invest* 115: 2702–2715, 2005. doi:10.1172/JCI24970.
12. **Clayburgh DR, Rosen S, Witkowski E, Wang FJ, Blair S, Dudek S, Garcia JG, Alverdy J, Turner JR.** A differentiation-dependent splice variant of myosin light chain kinase, MLCK1, regulates epithelial tight junction permeability. *FASEB J* 27: 55506–55513, 2005.
13. **Costantini TW, Loomis WH, Putnam JG, Kroll L, Eliceiri BP, Baird A, Bansal V, and Coimbra R.** Pentoxifylline modulates intestinal tight junction signaling after burn injury: effects on myosin light chain kinase. *J Trauma* 66: 17–24, 2009.
14. **Costantini TW, Peterson CY, Kroll L, Loomis WH, Eliceiri BP, Baird A, Bansal V, Coimbra R.** Role of p38 MAPK in burn-induced intestinal barrier breakdown. *J Surg Res* 156: 64–69, 2009. doi:10.1016/j.jss.2009.03.066.
15. **Cuenda A, Rousseau S.** p38 MAPKs pathway regulation, function and role in human diseases. *Biochim Biophys Acta* 1773: 1358–1375, 2007. doi:10.1016/j.bbamer.2007.03.010.
16. **Dubois B, Opendakker G, Carton H.** Gelatinase B in multiple sclerosis and experimental autoimmune encephalomyelitis. *Acta Neurol Belg* 99: 53–56, 1999.
17. **Dufour A, Zucker S, Sampson NS, Kuscu C, Cao J.** Role of matrix metalloproteinase-9 dimers in cell migration: design of inhibitory pep-

- tides. *J Biol Chem* 285: 35944–35956, 2010. doi:10.1074/jbc.M109.091769.
19. Eickelberg O, Sommerfeld CO, Wyser C, Tamm M, Reichenberger F, Bardin PG, Solèr M, Roth M, Perruchoud AP. MMP and TIMP expression pattern in pleural effusions of different origins. *Am J Respir Crit Care Med* 156: 1987–1992, 1997. doi:10.1164/ajrcm.156.6.9704112.
  20. Feighery LM, Cochrane SW, Quinn T, Baird AW, O'Toole D, Owens SE, O'Donoghue D, Mrsny RJ, Brayden DJ. Myosin light chain kinase inhibition: correction of increased intestinal epithelial permeability in vitro. *Pharm Res* 25: 1377–1386, 2008. doi:10.1007/s11095-007-9527-6.
  21. Gan X, Wong B, Wright SD, Cai TQ. Production of matrix metalloproteinase-9 in CaCO-2 cells in response to inflammatory stimuli. *J Interferon Cytokine Res* 21: 93–98, 2001. doi:10.1089/107999001750069953.
  22. Garg P, Vijay-Kumar M, Wang L, Gewirtz AT, Merlin D, Sitaraman SV. Matrix metalloproteinase-9-mediated tissue injury overrides the protective effect of matrix metalloproteinase-2 during colitis. *Am J Physiol Gastrointest Liver Physiol* 296: G175–G184, 2009. doi:10.1152/ajpgi.90454.2008.
  23. Guo S, Al-Sadi R, Said HM, Ma TY. Lipopolysaccharide causes an increase in intestinal tight junction permeability in vitro and in vivo by inducing enterocyte membrane expression and localization of TLR-4 and CD14. *Am J Pathol* 182: 375–387, 2013. doi:10.1016/j.ajpath.2012.10.014.
  24. Hollander D. Intestinal permeability, leaky gut, and intestinal disorders. *Curr Gastroenterol Rep* 1: 410–416, 1999. doi:10.1007/s11894-999-0023-5.
  25. Hollander D, Vadheim CM, Brettholz E, Petersen GM, Delahunty T, Rotter JL. Increased intestinal permeability in patients with Crohn's disease and their relatives. A possible etiologic factor. *Ann Intern Med* 105: 883–885, 1986. doi:10.7326/0003-4819-105-6-883.
  26. Ishida K, Takai S, Murano M, Nishikawa T, Inoue T, Murano N, Inoue N, Jin D, Umegaki E, Higuchi K, Miyazaki M. Role of chymase-dependent matrix metalloproteinase-9 activation in mice with dextran sodium sulfate-induced colitis. *J Pharmacol Exp Ther* 324: 422–426, 2008. doi:10.1124/jpet.107.131946.
  27. Itoh T, Matsuda H, Tanioka M, Kuwabara K, Itohara S, Suzuki R. The role of matrix metalloproteinase-2 and matrix metalloproteinase-9 in antibody-induced arthritis. *J Immunol* 169: 2643–2647, 2002. doi:10.4049/jimmunol.169.5.2643.
  28. Kennedy RJ, Hoper M, Deodhar K, Erwin PJ, Kirk SJ, Gardiner KR. Interleukin 10-deficient colitis: new similarities to human inflammatory bowel disease. *Br J Surg* 87: 1346–1351, 2000. doi:10.1046/j.1365-2168.2000.01615.x.
  29. Kirkegaard T, Hansen A, Bruun E, Brynskov J. Expression and localisation of matrix metalloproteinases and their natural inhibitors in fistulae of patients with Crohn's disease. *Gut* 53: 701–709, 2004. doi:10.1136/gut.2003.017442.
  30. Kobayashi K, Arimura Y, Goto A, Okahara S, Endo T, Shinomura Y, Imai K. Therapeutic implications of the specific inhibition of causative matrix metalloproteinases in experimental colitis induced by dextran sulphate sodium. *J Pathol* 209: 376–383, 2006. doi:10.1002/path.1978.
  31. Lapointe TK, Buret AG. Interleukin-18 facilitates neutrophil transmigration via myosin light chain kinase-dependent disruption of occludin, without altering epithelial permeability. *Am J Physiol Gastrointest Liver Physiol* 302: G343–G351, 2012. doi:10.1152/ajpgi.00202.2011.
  32. Liu H, Patel NR, Walter L, Ingersoll S, Sitaraman SV, Garg P. Constitutive expression of MMP9 in intestinal epithelium worsens murine acute colitis and is associated with increased levels of proinflammatory cytokine Kc. *Am J Physiol Gastrointest Liver Physiol* 304: G793–G803, 2013. doi:10.1152/ajpgi.00249.2012.
  33. Ma TY, Anderson JM. *Tight junctions and the intestinal barrier*. In: *Physiology of the Gastrointestinal Tract, 5th Edition*, edited by H. Said. Burlington, MA: Elsevier Academic Press, 2012. doi:10.1016/B978-0-12-382026-6.00038-5.
  34. Ma TY, Boivin MA, Ye D, Pedram A, Said HM. Mechanism of TNF-alpha modulation of Caco-2 intestinal epithelial tight junction barrier: role of myosin light-chain kinase protein expression. *Am J Physiol Gastrointest Liver Physiol* 288: G422–G430, 2005. doi:10.1152/ajpgi.00412.2004.
  35. Ma TY, Hoa NT, Tran DD, Bui V, Pedram A, Mills S, Merryfield M. Cytochalasin B modulation of Caco-2 tight junction barrier: role of myosin light chain kinase. *Am J Physiol Gastrointest Liver Physiol* 279: G875–G885, 2000. doi:10.1152/ajpgi.2000.279.5.G875.
  36. Ma TY, Iwamoto GK, Hoa NT, Akotia V, Pedram A, Boivin MA, Said HM. TNF- $\alpha$ -induced increase in intestinal epithelial tight junction permeability requires NF- $\kappa$ B activation. *Am J Physiol Gastrointest Liver Physiol* 286: G367–G376, 2004. doi:10.1152/ajpgi.00173.2003.
  37. Madara JL, Moore R, Carlson S. Alteration of intestinal tight junction structure and permeability by cytoskeletal contraction. *Am J Physiol* 253: C854–C861, 1987. doi:10.1152/ajpcell.1987.253.6.C854.
  38. Moore BA, Manthey CL, Johnson DL, Bauer AJ. Matrix metalloproteinase-9 inhibition reduces inflammation and improves motility in murine models of postoperative ileus. *Gastroenterology* 141: 1283–1292, 2011. doi:10.1053/j.gastro.2011.06.035.
  39. Mott JD, Werb Z. Regulation of matrix biology by matrix metalloproteinases. *Curr Opin Cell Biol* 16: 558–564, 2004. doi:10.1016/j.ceb.2004.07.010.
  40. Nighot P, Al-Sadi R, Rawat M, Guo S, Watterson DM, Ma T. Matrix metalloproteinase 9-induced increase in intestinal epithelial tight junction permeability contributes to the severity of experimental DSS colitis. *Am J Physiol Gastrointest Liver Physiol* 309: G988–G997, 2015. doi:10.1152/ajpgi.00256.2015.
  41. Paterson BM, Lammers KM, Arrieta MC, Fasano A, Meddings JB. The safety, tolerance, pharmacokinetic and pharmacodynamic effects of single doses of AT-1001 in coeliac disease subjects: a proof of concept study. *Aliment Pharmacol Ther* 26: 757–766, 2007. doi:10.1111/j.1365-2036.2007.03413.x.
  42. Peifer C, Wagner G, Laufer S. New approaches to the treatment of inflammatory disorders small molecule inhibitors of p38 MAP kinase. *Curr Top Med Chem* 6: 113–149, 2006. doi:10.2174/156802606775270323.
  43. Qiu L, Qian Y, Liu Z, Wang C, Qu J, Wang X, Wang S. Perfluorooctane sulfonate (PFOS) disrupts blood-testis barrier by down-regulating junction proteins via p38 MAPK/ATF2/MMP9 signaling pathway. *Toxicology* 373: 1–12, 2016. doi:10.1016/j.tox.2016.11.003.
  44. Rajashekhar G, Shivanna M, Kompella UB, Wang Y, Srinivas SP. Role of MMP-9 in the breakdown of barrier integrity of the corneal endothelium in response to TNF- $\alpha$ . *Exp Eye Res* 122: 77–85, 2014. doi:10.1016/j.exer.2014.03.004.
  45. Rodrigues DM, Sousa AJ, Hawley SP, Vong L, Gareau MG, Kumar SA, Johnson-Henry KC, Sherman PM. Matrix metalloproteinase 9 contributes to gut microbe homeostasis in a model of infectious colitis. *BMC Microbiol* 12: 105, 2012. doi:10.1186/1471-2180-12-105.
  46. Santana A, Medina C, Paz-Cabrera MC, Díaz-Gonzalez F, Farré E, Salas A, Radomski MW, Quintero E. Attenuation of dextran sodium sulphate induced colitis in matrix metalloproteinase-9 deficient mice. *World J Gastroenterol* 12: 6464–6472, 2006. doi:10.3748/wjg.v12.i40.6464.
  47. Turner JR. Molecular basis of epithelial barrier regulation: from basic mechanisms to clinical application. *Am J Pathol* 169: 1901–1909, 2006. doi:10.2353/ajpath.2006.060681.
  48. Turner JR, Rill BK, Carlson SL, Carnes D, Kerner R, Mrsny RJ, Madara JL. Physiological regulation of epithelial tight junctions is associated with myosin light-chain phosphorylation. *Am J Physiol* 273: C1378–C1385, 1997. doi:10.1152/ajpcell.1997.273.4.C1378.
  49. Vermaelen KY, Cataldo D, Tournoy K, Maes T, Dhulst A, Louis R, Foidart JM, Noël A, Pauwels R. Matrix metalloproteinase-9-mediated dendritic cell recruitment into the airways is a critical step in a mouse model of asthma. *J Immunol* 171: 1016–1022, 2003. doi:10.4049/jimmunol.171.2.1016.
  50. Wainwright MS, Rossi J, Schavocky J, Crawford S, Steinhorn D, Velentza AV, Zasadzki M, Shirinsky V, Jia Y, Haiech J, Van Eldik LJ, Watterson DM. Protein kinase involved in lung injury susceptibility: evidence from enzyme isoform genetic knockout and in vivo inhibitor treatment. *Proc Natl Acad Sci USA* 100: 6233–6238, 2003. doi:10.1073/pnas.1031595100.
  51. Wang Q, Guo XL, Wells-Byrum D, Noel G, Pritts TA, Ogle CK. Cytokine-induced epithelial permeability changes are regulated by the activation of the p38 mitogen-activated protein kinase pathway in cultured Caco-2 cells. *Shock* 29: 531–537, 2008. doi:10.1097/SHK.0b013e318150737f.
  52. Wild GE, Waschke KA, Bitton A, Thomson AB. The mechanisms of prednisone inhibition of inflammation in Crohn's disease involve changes in intestinal permeability, mucosal TNFalpha production and nuclear factor kappa B expression. *Aliment Pharmacol Ther* 18: 309–317, 2003. doi:10.1046/j.1365-2036.2003.01611.x.
  53. Wilson KP, Fitzgibbon MJ, Caron PR, Griffith JP, Chen W, McCaffrey PG, Chambers SP, Su MS. Crystal structure of p38 mitogen-activated protein kinase. *J Biol Chem* 271: 27696–27700, 1996. doi:10.1074/jbc.271.44.27696.

54. **Wyatt J, Vogelsang H, Hübl W, Waldhöer T, Lochs H.** Intestinal permeability and the prediction of relapse in Crohn's disease. *Lancet* 341: 1437–1439, 1993. doi:[10.1016/0140-6736\(93\)90882-H](https://doi.org/10.1016/0140-6736(93)90882-H).
55. **Ye D, Ma I, Ma TY.** Molecular mechanism of tumor necrosis factor- $\alpha$  modulation of intestinal epithelial tight junction barrier. *Am J Physiol Gastrointest Liver Physiol* 290: G496–G504, 2006. doi:[10.1152/ajpgi.00318.2005](https://doi.org/10.1152/ajpgi.00318.2005).
56. **Ye D, Ma TY.** Cellular and molecular mechanisms that mediate basal and tumour necrosis factor-alpha-induced regulation of myosin light chain kinase gene activity. *J Cell Mol Med* 12: 1331–1346, 2008. doi:[10.1111/j.1582-4934.2008.00302.x](https://doi.org/10.1111/j.1582-4934.2008.00302.x).
57. **Zhang J, Shen B, Lin A.** Novel strategies for inhibition of the p38 MAPK pathway. *Trends Pharmacol Sci* 28: 286–295, 2007. doi:[10.1016/j.tips.2007.04.008](https://doi.org/10.1016/j.tips.2007.04.008).
58. **Zhang Y, Li J, Chi Y, Li M, Pan X, Zhang Q, He X, Liu Y.** [Myosin light chain kinase involved in change of intestinal mucosal barrier function in nonalcoholic steatohepatitis mice model]. *Zhonghua Nei Ke Za Zhi* 54: 434–438, 2015.

